Egypt. J. Chem. **Vol. 64,** No. 8 pp. 3981 - 3989 (2021)

Egyptian Journal of Chemistry

http://ejchem.journals.ekb.eg/

Modelling for removal of Cr(VI) and Pb(II) using sago bark (Metroxylon sagu) by fixed-bed column method

Syiffa Fauzia[1], Hermansyah Aziz[2], Dahyunir Dahlan[3], Rahmiana Zein[1]*

[1]*Laboratory of Analytical Environmental Chemistry, Department of Chemistry,Andalas University, 25163, Padang, Indonesia*

[2]*Laboratory of Physical Chemistry, Department of Chemistry, Andalas University, 25163, Padang, Indonesia*

[3]*Laboratory of Material and Structure, Department of Physics, Andalas University, Padang, 25163, Indonesia*

Abstract

Industries commonly produced a large scale of wastewater that consisted of hazardous materials such heavy metals. Recently, one of popular methods for wastewater treatment was adsorption system using biosorbent. Sago bark (*Metroxylon sagu*) was a solid waste remained from sago starch industry. It contained various functional group such as carbonyl and hydroxyl groups that could be utilized to resolve wastewater containing metal ions. Removal of Cr(VI) and Pb(II) using sago bark (*Metroxylon sagu*) have been investigated by a fixed bed column reactor. The effect of flow rate (2, 4, 6 mL/min) and bed depth (3, 6, 9 cm) was examined in order to observe column performance (15x1 cm id). The result revealed that the lower flow rate and the higher bed depth delayed the breakthrough time and exhaustion time. Thus, the optimum conditions were achieved at 2 mL/min of flow rate and 9 cm of bed depth for both metal ions. The equation of Thomas, BDST and Yoon-Nelson models was carried out to evaluate the breakthrough curve. The repeatability and regeneration of sago bark were analyzed by HNO_3 0.01 M within 3 cycles. It means that sago bark has a promising ability to remove Cr(VI) and Pb(II) ions in solution.

Keywords: adsorption; column continuous; Cr(VI); Pb(II); sago bark

1. Introduction

Industrial growth has been contributed to environmental issue due to the generation of either liquid or solid waste as secondary product after industrial processing. Approximately, 1.15 tons waste produced were not processed in Indonesia [1]. Recently, heavy metal waste has become a threat to the wide world. Heavy metal exposure is able to defect the environment, animals, and human. These heavy metals enter the human body through the food chain, water or other daily activities. Heavy metal such as lead (Pb(II)) and chromium (Cr(VI)) is presented in various industries like tanning, mining, batteries, electroplating, paint and so forth [2]. Pb(II) gather in the body and poison biological activities of living organism that harm kidney, liver, and etcetera. Whereas, chromium in Cr(VI) oxidation state is highly soluble rather than Cr(III) oxidation state. Cr(VI) forms a hexavalent chromium ion that highly toxic due to its mobility that causes a mutagenic, carcinogenic and other harmful diseases [3–5]. Considering its negative effect, various methods have been conducted to treat heavy metal wastewater so that it is feasible to be discharged to the environment. One of them is adsorption. Adsorption is an accumulation of compound in the liquid/gas phase on the solid surface. This method utilizes an adsorbent commonly come from waste such as agricultural waste or biomass for example pensi shell [6], *Neplhelium lappaceum* [7], *Macrocystis pyrifera* and *Undaria pinnatifida* [8], *Swietenia Mahogani* fruit shells [9], oil palm fibre [10], immobilized citrus peels [11], residue allspice [12] and so forth. All of the adsorbent mentioned above own the advantages of adsorption method. It is low cost, easy to prepare, no secondary waste, efficient for the low metal ion concentration, and simple [9, 12]. The adsorption of Cr(VI) and Pb(II) using sago bark (*Metroxilon sagu*) has been performed by previous research employing the batch system [13, 14]. The batch system provides information regarding the

* *Corresponding author: rzein@sci.unand.ac.id or mimiedison@yahoo.co.id*

Receive Date: 27 November 2019, Revise Date: 02 April 2020, Accept Date: 08 April 2021

DOI: 10.21608/EJCHEM.2020.20172.2212

equilibrium and kinetic mechanism. Unfortunately, this system is unable to be applied to industrial purpose because the volume treated is constant/limited giving lower driving force and the gradient concentration does not exist **[5, 15].** Therefore, the column system is required to evaluate the adsorbent efficiency through the breakthrough curve shape. The breakthrough performance implies the probability of adsorbent for industrial application [8, 9, 12]. The previous research utilized stem tree of soybean to remove Pb(II) and Zn(II) has applied optimum condition that was obtained from batch system in continuous flow system. The adsorption capacity for both Pb(II) and Zn(II) was 12.44 mg/g and 6.75 mg/g, respectively [16]. Beside, sago bark was a solid waste from sago starch industry which generated about 1.5 tons waste per day [17]. Therefore, it becomes a concern to overcome this problem as well. The purpose of the present research is to investigate the efficiency of sago bark for Cr(VI) and Pb(II) removal in fixed bed column. Some parameters are subjected to evaluate the adsorbent performance such as flow rate and bed depth. The breakthrough curve is described by Thomas, BDST and Yoon-Nelson models.

2. Experimental Section

Material and Adsorbent preparation

Pb(II) and Cr(VI) solution were prepared by dissolving $Pb(NO_3)_2$ and $K_2Cr_2O_7$ in distilled water. NaOH or HCl was used to adjust solution pH. HNO_3 was employed as chemical activator of adsorbent and glass wool. All the reagents were analytical grade purchased by Merk, Germany. Sago bark (Metroxylon sagu) was collected from the local area, West Sumatra, Indonesia. The sample was washed to remove dirt and then sundried. Dried sago bark was crushed to get fine size <160 µm. Sago bark powder was soaked in 0.01 M HNO_3 for an hour. Then, filtered and rinsed with distilled water until neutral pH. The powder was sundried to remove water.

Fixed bed column procedure

The fixed-bed column was carried out in a glass column (15 cm length and 1 cm inner diameter). Some parameters were studied to evaluate fixed-bed column performance such as flow rate (2, 4, 6 mL/min), adsorbent mass (0.5;1;1.5 g), and adsorption-desorption cycles. pH and initial concentration of metal ions have been studied in the batch system. These optimum conditions were employed to evaluate the ability of sago bark in column system since dynamic system more practical in industry. Optimum conditions of Cr(VI) in the batch system were achieved at pH 3 and 1000 mg/L of Cr(VI) concentration [14]. Whereas Pb(II) reached the peak at pH 5 and 800 mg/L of Pb(II) concentration [13].

In the bottom of a column, glass wool was attached to prevent adsorbent loss during adsorption. The metal solution was pumped by a peristaltic pump. The effluent was collected every 5 minutes for an hour. Metal ion concentration was measured by AAS (Atomic Absorption Spectrophotometer). The breakthrough time and exhaustion time were observed by plotting Ce/Co Vs time (breakthrough curve). Sago bark was characterized by FTIR (Fourier Transform Infra-Red), SEM (Scanning Electron Microscopy), and BET (Bruener Emmet-Teller).

Column adsorption data modelling

Thomas model

The linearization of the Thomas model was derived by plotting $\ln\left(\frac{C_o}{C_t}-1\right)$ vs t. Thomas model stated that the adsorption process was reversible based on the second-order kinetic model with no axial dispersion [5, 18]. This model was represented by the following equation:

$$\ln\left(\frac{C_o}{C_t}-1\right) = \frac{k_{TH}q_o\,m}{Q} - k_{TH}C_o t \qquad \text{Equation (1)}$$

Where Co and Ct were initial concentration and concentration of metal ion (mg/L) at the time (t). k_{TH} was Thomas model constant (L/mg.min). q_o and m were maximum adsorption (mg/g) and adsorbent mass (g), respectively. Meanwhile, Q was flow rate (mL/min).

Yoon-Nelson

This model gave information regarding the time required for 50 % breakthrough. This model was simple due to no detailed parameters needed. The Yoon-Nelson model was expressed by the given equation:

$$\ln\left(\frac{C_o}{C_o-C_t}\right) = k_{YN}t - k_{YN}\tau \qquad \text{Equation (2)}$$

Where k_{YN} and τ were Yoon-Nelson constant (min^{-1}) and time required at 50 % of breakthrough (min) [18, 19].

BDST (Bed depth service time)

BDST model can be employed to the adsorption process without further experiment. It can predict the service time of adsorbent before it has to be regeneration or replaced, the ability of adsorbent to adsorb the certain amount of adsorbate [5, 18]. The relationship of each parameter was determined by the following equat nion:

$$t = \frac{N_o Z}{C_o u} - \frac{1}{K_a C_o}\ln\left[\frac{C_0}{C_b}-1\right] \qquad \text{Equation (3)}$$

Where N_o and Z were bed adsorption capacity (mg/L) and bed height (cm), respectively. K_a was BDST model rate constant (L/mg/min), u was the linear

velocity (cm/min), t was service time (min) and C_b was the concentration at the breakthrough (mg/L).

3. Results And Discussion

Adsorbent characterization

The bark surface is observed by FTIR and SEM. FTIR spectra give spectra of functional groups existing in sago bark. The FTIR spectra of sago bark are given in figure 1. It showed that spectra range from 3650 to 3200 cm^{-1} indicated the hydroxyl group (O-H). The band within the range 3000-2850 cm^{-1} suggested the C-H stretching. The peak at 1740-1600 cm^{-1} represented the carbonyl group (C=O) and the peak at 1640-1550 cm^{-1} corresponded N-H bending (amine group). The hydroxyl and carbonyl group were contributed to form a complexation with Pb(II) by sharing their electron. Whereas, amine group (N-H) was considered to react with Cr(VI) [20]. Those were the common functional groups that ruled the adsorption process. The wavenumber of those functional group was shifted after contacting with Pb(II) and Cr(VI) ions marking the adsorption process occurred [21]. The SEM micrograph confirmed that the sago bark has a porous surface that supported the adsorption process to trap the metal ions on the surface and reduce the concentration of metal ion in the solution. After the adsorption process, the rough surface of sago bark changed. It became smoother and the availability of pores fell off (figure 2) [13, 14, 22]. According to BET analysis, the pore diameter of sago bark was 55.39 Å with the surface area of 4.845 m^2/g. This pore was able to tie the metal ions since Cr(VI) (ionic radii 80 pm=0.8 Å) and Pb(II) (ionic radii 119 pm=1.19 Å) have smaller ion radii [13, 14]. The efficiency of sago bark was affected by the metal ions properties as well such as the electronegativity, ionic radii, hydrated ion radii and so forth. These metal properties were contributed to the interaction between an adsorbent and metal ion either physical or chemical sorption [2, 13, 14, 23].

Flow rate effect

Effect of flow rate was carried out based on optimum condition obtain in a batch system (pH 3, initial concentration 1000 mg/L and pH 5, initial concentration 800 mg/L). The bed-depth was kept constant at 6 cm (1 g). The breakthrough curve of Cr(VI) and Pb(II) sorption were given in figure 3. It could be observed that breakthrough time (t_b) and exhaustion time (t_e) became shorter as the flow rate increased for both metal ions. The longer breakthrough time, the longer adsorbent can be used before it became saturated and has to be replaced or regenerated. Exhaustion time ($\mathbf{t_e}$) of Cr(VI) sorption decrease from 15 minutes at 2 mL/min of flow rate to 5 minutes at 6 mL/min of flow rate. The breakthrough of Pb(II) sorption showed that lower flow rate (2 mL/min) could delay exhaustion time up to 15 minutes and 6 mL/min of flow rate accelerated the exhaustion time to 5 minutes. The removal efficiency of sago bark for Cr(VI) removal from the lower to the higher flow rate was 92.86 %, 89.55 %, and 79.60 %, respectively. While the removal of Pb(II) with sago bark showed a reduction from 92.75 % to 79.50 % when the flow rate increased from 2 mL/min to 6 mL/min (table 1). Fast saturation time was induced by the short residence time of metal ion in contacting with adsorbent due to the higher flow rate. Metal ions left the column before adsorption was complete and reached equilibrium [24–26]. Moreover, the higher flow rate decreased the external of mass transfer resistance leading the saturation of adsorbent [27, 28]. Therefore, the lower flow rate (2 mL/min) was chosen for further use. The previous research also found the same result [10, 24, 25].

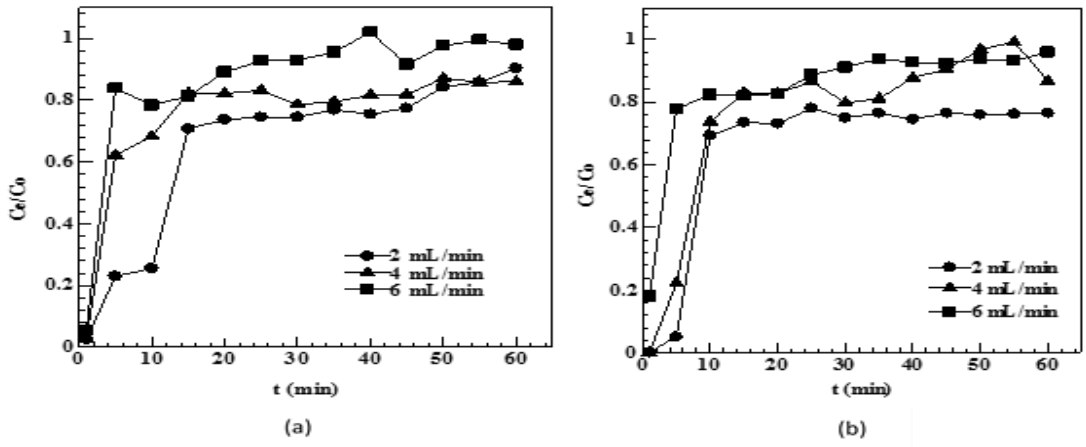

Figure 3. Breakthrough curve for adsorption of (a) Cr(VI) and (b) Pb(II) at different flow rate

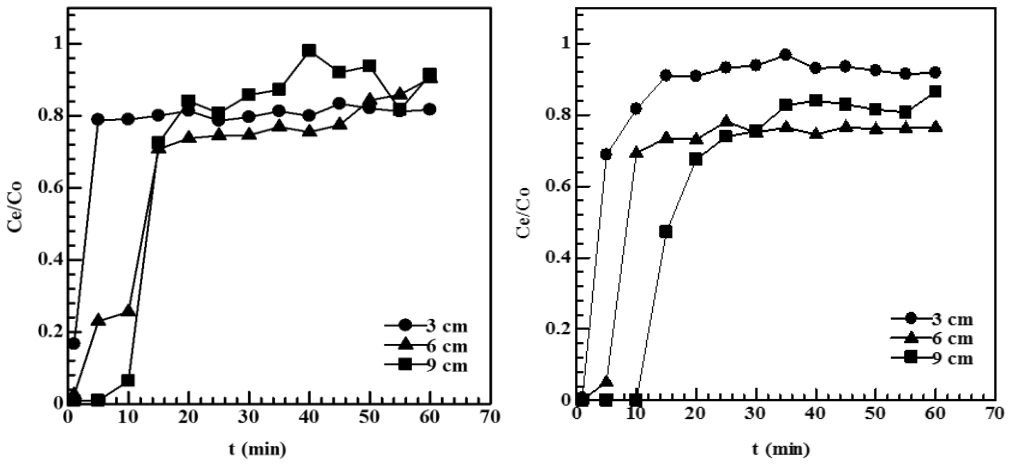

Figure 4. Breakthrough curve for adsorption of (a) Cr(VI) and (b) Pb(II) at different bed-depth

Bed depth effect

Figure 4 represented the breakthrough curve for Cr(VI) and Pb(II) sorption carried out at flow rate 2 mL/min and various bed depth 3 cm (0.5 g), 6 cm (1 g) and 9 cm (1.5 g) for each metal ions. The initial concentration and pH solution were kept constant at 1000 mg/L, pH 3 for Cr(VI) and 800 mg/L and pH 5 for Pb(II), respectively. It exhibited that longer bed-depth was able to delay breakthrough time (t_b) and exhaustion time (t_e). At highest bed-depth, Cr(VI) sorption achieved the breakthrough time (t_b) at 10 minutes and became exhausted after 20 minutes.

Meanwhile, Pb(II) sorption reached breakthrough time (t_b) and exhaustion time (t_e) after 10 minutes and 30 minutes, respectively at the highest bed-depth as well. Since the longer bed depth gave enough time for metal ions to diffuse into sago bark pore, it increased the opportunity of metal ions to interact with active site existed in sago bark [29]. Furthermore, as bed depth increased, the surface area increased providing a lot of active site to bind metal ion [30–32]. The adsorption efficiency of sago bark was 19.90 mg/g for Cr(VI) and 21.20 mg/g for Pb(II). The adsorption capacity for Pb(II) ion was higher than Cr(VI) ion because the electronegativity, ionic radii, hydrated ion radii of each metal ions. The electronegativity of Pb(II) (2.33) > Cr(VI) (1.66). This behaviour strongly assisted the interaction between functional group existing in adsorbent such as O-H (hydroxyl group) and C-O (carbonyl group) to form a complexion, ion exchange or electrostatic interaction [2, 23].

Application of column mathematical model

The data of column adsorption were executed by Thomas, Yoon-Nelson and BDST model. Table 3 showed the parameters involved in Thomas and Yoon-Nelson models. The Thomas constant (K_{TH}) decreased when the flow rate and the bed depth increased. It revealed that the q_o predicted by Thomas close to q_e obtained from experiment (table 1). This suggested that Thomas model was suited to describe the mechanism of Cr(VI) and Pb(II) removal using sago bark. It represented that external and internal diffusion were not rate limiting step [33]. The Yoon-Nelson constant (K_{YN}) is given in table 3 and 4. The Yoon-Nelson constant (K_{YN}) increased as the flow rate and bed depth increased. The time required for 50 % breakthrough (τ) declined at the higher flow rate. In reverse, when bed depth increased from 3 to 9 cm, the time required for 50 % breakthrough (τ) increased as well. This result indicated that the higher bed depth provided the longer mass transfer zone delaying the adsorbent sauration [19]. Whereas, The BDST model revealed a good agreement (R^2) for both metal ions indicating the external mass transfer dominance (table 4) [5].

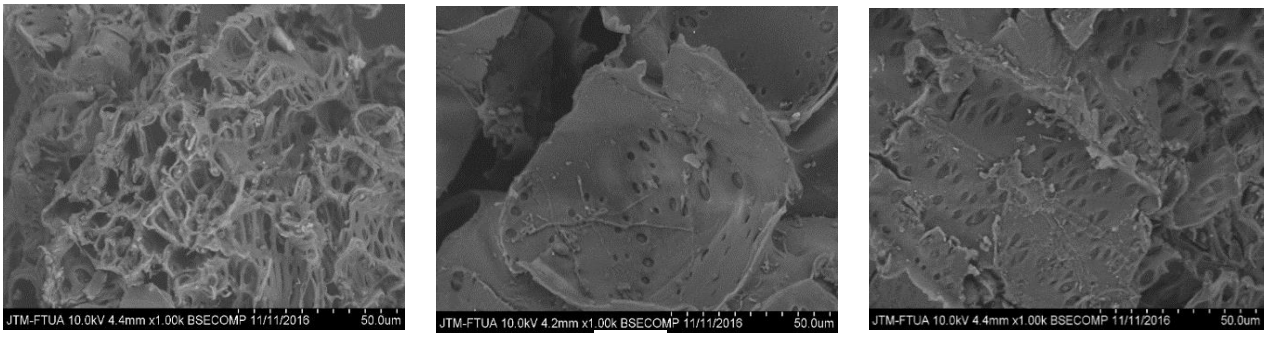

Figure 2. SEM image of sago bark (a) before sorption and after (b) Pb(II) sorption; (c) Cr(VI) sorption, magnification 1000 times

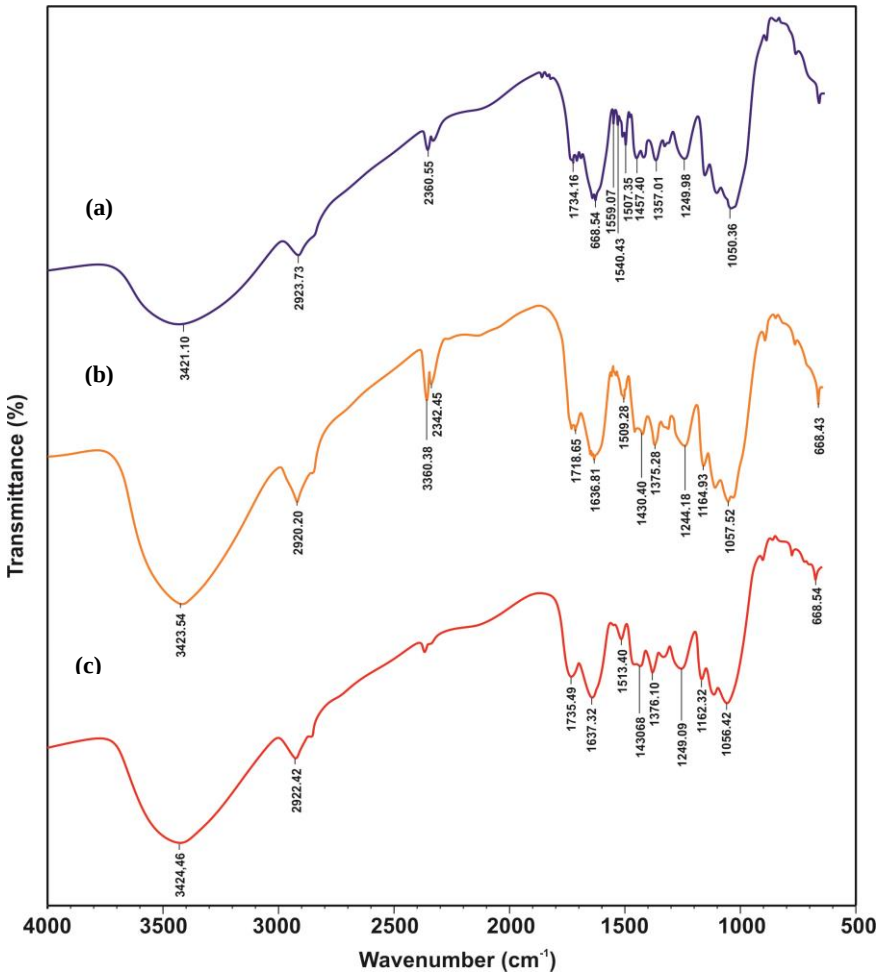

Figure 1. FTIR spectra of sago bark (a) before sorption and after (b) Pb(II);(c) Cr(VI) sorption

Adsorption desorption cycles

The adsorption-desorption study was conducted to evaluate the repeatability of adsorbent after several times. The resistance of adsorbent will determine the cost during wastewater treatment. The desorption of metal ions from sago bark was performed by HNO_3 0.01 M. The bed depth was 9 cm (1.5 g) with inlet concentration 800 mg/L for Pb(II) and 1000 mg/L for Cr(VI). The metal solution streamed down the column at 2 mL/min of flow rate and the outlet was collected every 5 minutes. The distilled water was employed to remove the residual acid. Figure 5 revealed the repeatability of sago bark on Pb(II) and Cr(VI) sorption. It can be seen that the breakthrough time and

exhaustion time was shorter after the third cycles. The adsorption capacity of sago bark declined from 26.50 mg/g at the first cycle to 16.53 mg/g at the third cycles for Pb(II). Whereas, for Cr(VI) the adsorption capacity went down from 19.90 mg/g to 4.79 mg/g at the first and the third cycles, respectively (table 2). The decrease in adsorption capacity is related to the saturation of active site to adsorb metal ions. Although the desorption process has performed by HNO_3 0.01 as a desorbing agent, there were the ions that were chemically attached on active site resulting in the number of vacant surfaces remains less. Therefore, the adsorption capacity decreased [33].

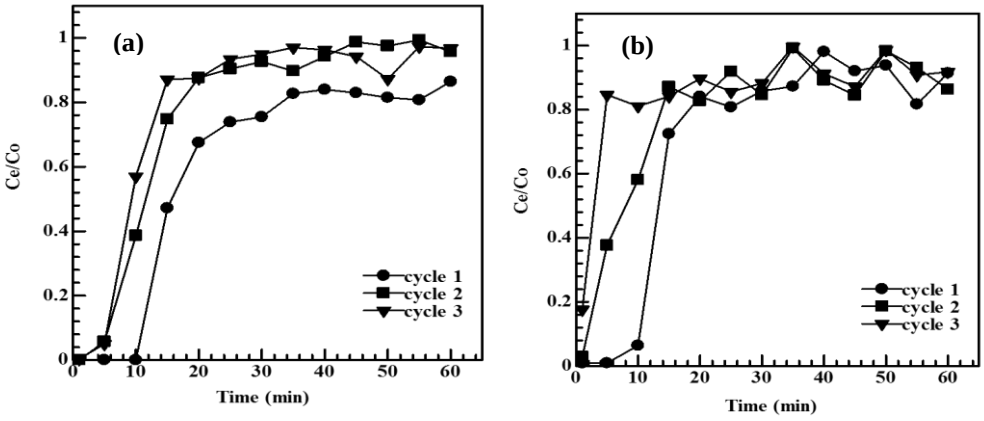

Figure 5. Adsorption-desorption cycle of (a)Pb(II) and (b) Cr(VI) on sago bark

Table 1.Cr(VI) and Pb(II) sorption parameters in a fixed bed column

Metal ion	Flow rate (mL/min)	Bed depth (cm)	t_b (min)	t_e (min)	AER (g/L)	EBRT (s)	BV	MTZ (cm)	Ce (mg/L)	q_{total} (mg)	m_{total} (mg)	q_e (mg/g)	RE (%)
Cr(VI)	2	6	1	15	33.33	12.73	0.42	5.6	71.33	27.86	30	27.86	92.86
	4	6	1	10	25	12.73	0.84	5.4	104.5	35.82	40	35.82	89.55
	6	6	1	5	33.33	12.73	1.27	4.8	204	23.88	30	23.88	79.60
	2	3	1	5	50	25.47	0.84	2.4	204	7.96	10	15.92	79.60
Pb(II)	2	6	1	15	33.33	12.73	0.42	5.6	72.66	27.82	30	27.82	92.73
	2	9	10	20	37.50	84.92	2.83	4.5	253.75	29.85	40	19.90	74.62
	2	6	1	15	33.33	12.73	0.42	5.6	58	22.26	24	22.26	92.75
	4	6	1	10	25	12.73	0.84	5.4	84.50	28.62	32	28.62	89.43
	6	6	1	5	33.33	12.73	1.27	4.8	164	19.08	24	19.08	79.50
	2	3	1	5	50	25.47	0.84	2.4	126	6.74	8	13.48	84.25
	2	6	1	15	33.33	12.73	0.42	5.6	58	22.26	24	22.26	92.75
	2	9	10	30	25	84.92	2.83	6	270	31.80	48	21.20	66.25

Table 2. Adsorption capacity of sago bark after adsorption desorption cycles

Metal ion	Number of cycle	Flow rate (mL/min)	Bed depth (cm)	t_b (min)	t_e (min)	AER (g/L)	EBRT (s)	BV	MTZ (cm)	Ce (mg/L)	q_{total} (mg)	m_{total} (mg)	q_e (mg/g)	RE (%)
Cr(VI)	1	2	9	10	25	30	127.38	4.24	5.4	403	29.85	50	19.90	59.70
	2	2	9	1	15	50	12.73	0.42	8.4	161	25.17	30	16.78	83.90
	3	2	9	1	5	150	12.73	0.42	7.2	281	7.19	10	4.79	71.90
Pb(II)	1	2	9	10	35	21.42	127.38	4.24	6.42	232.14	39.75	56	26.50	70.98
	2	2	9	5	25	30	63.69	2.12	7.20	138.60	33.07	40	22.04	82.67
	3	2	9	5	20	37.50	63.69	2.12	6.75	180	24.08	32	16.53	77.50

Table 3. Thomas and Yoon-Nelson model parameters at different flow rate and bed depth for Cr(VI) and Pb(II) removal

Metal ions	Flow rate (mL/min)	Z (cm)	Thomas			Yoon-Nelson		
			K_{TH} (L/mg.min)	q_o (mg/g)	R^2	K_{YN} (min^{-1})	τ (min)	R^2
Cr(VI)	2	6	$2.85x10^{-4}$	24.02	0.8892	0.2852	12.01	0.8892
	4	6	$3.46x10^{-4}$	32.52	0.7607	0.3465	8.12	0.7607
	6	6	$3.77x10^{-4}$	36.58	0.6241	0.4377	5.26	0.6241
	2	3	$1.83x10^{-4}$	17.78	0.5677	0.1830	4.45	0.5677
	2	6	$2.85x10^{-4}$	24.02	0.8892	0.2852	12.01	0.8892
	2	9	$4.53x10^{-4}$	20.15	0.9454	0.4537	15.11	0.9454
Pb(II)	2	6	$6.61x10^{-4}$	17.81	0.8902	0.5281	11.13	0.8902
	4	6	$6.52x10^{-4}$	34.69	0.8307	0.5593	10.12	0.8307
	6	6	$6.52x10^{-4}$	34.69	0.8307	0.5593	10.12	0.8307
	2	3	$4.14x10^{-4}$	18.68	0.7790	0.3552	3.63	0.7790
	2	6	$5.25x10^{-4}$	27.69	0.7311	0.4601	7.89	0.7311
	2	9	$6.61x10^{-4}$	17.81	0.8902	0.5281	11.13	0.8902

Table 4. BDST parameters for Cr(VI) and Pb(II) removal

Metal ions	BDST		
	No (mg/L)	Ka (L/mg.min)	R^2
Pb(II)	8489.39	$-6.082x10^{-5}$	0.9868
Cr(VI)	6366.75	$2.441x10^{-4}$	0.9643

4. Conclusion

The result revealed that the lower flow rate and the higher bed depth delayed the breakthrough time and exhaustion time. The optimum conditions were achieved at 2 mL/min of flow rate and 9 cm of bed depth for both metal ions. The breakthrough curve was properly explained by Thomas, Yoon-Nelson, and BDST model. The sago bark was successfully regenerated using HNO_3 0.01 M. It means that sago bark has a promising ability to remove Cr(VI) and Pb(II) ions in solution.

5. Conflict of Interest

The authors declare no conflicts of interest.

6. Acknowledgements

The authors are grateful to the Ministry of Research Technology and Higher Education of the Republic of Indonesia for the financial support. No. Agreement: 059/SP2H/LT/DPRM/IV/2017.

7. References

1. Aloysius V., and Daihani D.U., Closing The Waste Gap In Indonesia : Harnessing Industrial Waste To Prevent Pollution And Conserve Non-Renewable Resources. In Maastrich School of Management pp. 1–15 (2011).
2. Adhiambo O.R., Lusweti K.J., and Zachary G., Biosorption of Pb 2 + and Cr 2 + Using Moringa Oleifera and Their Adsorption Isotherms. *Science Journal of Analytical Chemistry*, **3**(6), 100–108 (2015).
3. Albadarin A.B., Mangwandi C., Al-Muhtaseb A.H., Walker G.M., Allen S.J., and Ahmad M.N.M., Modelling and fixed bed column adsorption of Cr(VI) onto orthophosphoric acid-activated lignin. *Chinese Journal of Chemical Engineering*, **20**(3), 469–477 (2012).
4. Gupta S., and Babu B. V, Experimental Investigations and Theoretical Modeling Aspects in Column Studies for Removal of Cr(VI) from Aqueous Solutions Using Activated Tamarind Seeds. *J Water Resource and Protection*,

2(August), 706–716 (2010).
5. Mohan S., Singh D.K., Kumar V., and Hasan S.H., Modelling of fixed bed column containing graphene oxide decorated by MgO nanocubes as adsorbent for Lead(II) removal from water. *Journal of Water Process Engineering*, **17**, 216–228 (2017).
6. Zein R., Syukri S., Muhammad M., Pratiwi I., and Yutaro D.R., The ability of Pensi (Corbicula moltkiana) shell to adsorb Cd(II) and Cr(VI) ions. In AIP Conference Proceedings pp. 1–8 (2018).
7. Zein R., Astuti A.W., Wahyuni D., Furqani F., and Munaf E., Removal of Methyl Red from Aqueous Solution by Neplhelium lappaceum . *Research Journal of Pharmaceutical , Biological and Chemical Sciences*, **6**(3), 86–97 (2015).
8. Plaza J., Marisa C., and Edgardo V., Dynamic Cr (III) uptake by Macrocystis pyrifera and Undaria pinnatifida biomasses. *Electronic Journal of Biotechnology*, **16**(3), 1–8 (2013).
9. Rangabhashiyam S., Suganya E., and Selvaraju N., Packed bed column investigation on hexavalent chromium adsorption using activated carbon prepared from *Swietenia Mahogani* fruit shells. *Desalination and Water Treatment*, (August), 1–8 (2015).
10. Nwabanne J.T., and Igbokwe P.K., Adsorption Performance of Packed Bed Column for the removal of Lead (ii) using oil Palm Fibre. *International Journal of Applied Science and TEchnology*, **2**(5), 106–115 (2012).
11. Chatterjee A., and Schiewer S., Multi-resistance kinetic models for biosorption of Cd by raw and immobilized citrus peels in batch and packed-bed columns. *Chemical Engineering Journal*, **244**, 105–116 (2014).
12. Cruz-olivares J., Pérez-alonso C., Barrera-díaz C., Ureña-nuñez F., and Chaparro-mercado M.C., Modeling of lead (II) biosorption by residue of allspice in a fixed-bed column. *Chemical Engineering Journal*, **228**, 21–27 (2013).
13. Fauzia S., Aziz H., Dahlan D., and Zein R., Study of Equilibrium , Kinetic and Thermodynamic for Removal of Pb (II) in Aqueous Solution Using Sago Bark (Metroxylon sago). *AIP Conference Proceedings*, **2023**(020081), 1–8 (2018).
14. Fauzia S., Aziz H., Dahlan D., Namiesnik J., and Zein R., Adsorption of Cr (VI) in aqueous solution using sago bark (Metroxylon sagu) as a new potential biosorbent. *Desalination and Water Treatment*, **147**, 191–202 (2019).
15. Abdolali A., Ngo H.H., Guo W., Zhou J.L., Zhang J., Liang S., *et al.*, Application of a breakthrough biosorbent for removing heavy metals from synthetic and real wastewaters in a lab-scale continuous fixed-bed column. *Bioresource Technology*, **229**(January), 78–87 (2017).
16. Harmiwati, Salmariza, Kurniawati D., Lestari I., Chaidir Z., Desmiarti R., *et al.*, Biosorption of Pb(II) and Zn(II) metal ions from aqueous solution by stem tree of soyben using continuous flow method. *ARPN Journal of Engineering and Applied Sciences*, **12**(18), 5258–5262 (2017).
17. Awg-Adeni D.S., Abd-Aziz S., Bujang K., and Hassan M.A., Bioconversion of sago residue into value added products. *African Journal of Biotechnology*, **9**(14), 2016–2021 (2016).
18. Rout P.R., Dash R.R., and Bhunia P., Modelling and packed bed column studies on adsorptive removal of phosphate from aqueous solutions by a mixture of ground burnt patties and red soil. *Advances in Environmental Research*, **3**(3), 231–251 (2014).
19. Fadzil F., Ibrahim S., Ahmad M., and Megat K., Adsorption of lead (II) onto organic acid modified rubber leaf powder : Batch and column studies. *Process Safety and Environmental Protection*, **100**, 1–8 (2015).
20. Li H., Dong X., Evandro B., Oliveira L.M. De, Chen Y., and Ma L.Q., Mechanisms of metal sorption by biochars : Biochar characteristics and modifications. *Chemosphere*, **178**, 466–478 (2017).
21. Moyo M., Chikazaza L., Nyamunda B.C., and Guyo U., Adsorption Batch Studies on the Removal of Pb (II) Using Maize Tassel Based Activated Carbon Adsorption Batch Studies on the Removal of Pb (II) Using. *Journal of chemistry*, 1–8 (2013).
22. Biswas S., and Mishra U., Continuous Fixed-Bed Column Study and Adsorption Modeling : Removal of Lead Ion from Aqueous Solution by Charcoal Originated from Chemical Carbonization of Rubber Wood Sawdust. *Journal of chemistry*, 1–9 (2015).
23. Hannachi Y., Ghorbel A., Lasram T., and Boubaker T., Removal of Ni(II) ions from aqueous solutions using clinoptilolite: Equilibrium, kinetic and thermodynamic studies. *Chemistry and Ecology*, (October 2014), 1–15 (2012).
24. Chao H.P., Chang C.C., and Nieva A., Biosorption of heavy metals on Citrus maxima peel, passion fruit shell, and sugarcane bagasse in a fixed-bed column. *Journal of Industrial and Engineering Chemistry*, **20**(5), 3408–3414 (2014).
25. Lim A.P., and Aris A.Z., Continuous fixed-bed column study and adsorption modeling: Removal of cadmium (II) and lead (II) ions in aqueous solution by dead calcareous skeletons. *Biochemical Engineering Journal*, **87**, 50–61 (2014).
26. Sulaymon A.H., Yousif S.A., and Al-Faize M.M.,

Competitive biosorption of lead mercury chromium and arsenic ions onto activated sludge in fixed bed adsorber. *Journal of the Taiwan Institute of Chemical Engineers*, **45**(2), 325–337 (2014).
27. Mondal N.K., Bhaumik R., Roy P., Das B., and Datta J.K., Investigation on fixed bed column performance of fluoride adsorption by sugarcane charcoal. *Journal of Environmental Biology*, **34**, 1059–1064 (2013).
28. Maheshwari U., and Gupta S., Performance evaluation of activated neem bark for the removal of Zn(II) and Cu(II) along with other metal ions from aqueous solution and synthetic pulp & paper industry effluent using fixed-bed reactor. *Process Safety and Environmental Protection*, **102**(Ii), 547–557 (2016).
29. Shanmugaprakash M., and Sivakumar V., Batch and fixed-bed column studies for biosorption of Zn(II) ions onto pongamia oil cake (Pongamia pinnata) from biodiesel oil extraction. *Journal of Environmental Management*, **164**, 161–170 (2015).
30. Calero M., Hernáinz F., Blázquez G., Tenorio G., and Martín-Lara M.A., Study of Cr (III) biosorption in a fixed-bed column. *Journal of Hazardous Materials*, **171**(1–3), 886–893 (2009).
31. Sharma R., and Singh B., Removal of Ni (II) ions from aqueous solutions using modified rice straw in a fixed bed column. *Bioresource Technology*, **146**, 519–524 (2013).
32. Chen S., Yue Q., Gao B., Li Q., Xu X., and Fu K., Adsorption of hexavalent chromium from aqueous solution by modified corn stalk: A fixed-bed column study. *Bioresource Technology*, **113**, 114–120 (2012).
33. Zang T., Cheng Z., Lu L., Jin Y., Xu X., Ding W., *et al.*, Removal of Cr(VI) by modified and immobilized Auricularia auricula spent substrate in a fixed-bed column. *Ecological Engineering*, **99**, 358–365 (2017).